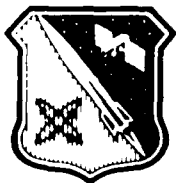


MICROCOPY RESOLUTION TEST CHART
NATIONAL BUREAU OF STANDARDS - 1963-A

9



AFAL TR-87-061

AD:

DTIC FILE COPY

Special Report
for the period
September 1986 to
March 1987

Durability Testing of an Iridium-Plated Storable Rocket Engine Injector

September 1987

Author:
K. R. Benson, Capt, USAF

AD-A190 707

Approved for Public Release

Distribution is unlimited. The AFAL Technical Services Office has reviewed this report, and it is releasable to the National Technical Information Service, where it will be available to the general public, including foreign nationals.

DTIC
ELECTE
JAN 19 1988
S H D

Air Force Astronautics Laboratory

Air Force Space Technology Center
Space Division, Air Force Systems Command
Edwards Air Force Base,
California 93523-5000

88 1 19 1987

NOTICE

When U.S. Government drawings, specifications, or other data are used for any purpose other than a definitely related Government procurement operation, the fact that the Government may have formulated, furnished, or in any way supplied the said drawings, specifications, or other data, is not to be regarded by implication or otherwise, or in any way licensing the holder or any other person or corporation, or conveying any rights or permission to manufacture, use, or sell any patented invention that may be related thereto.

FOREWORD

This special report documents the Air Force Astronautics Laboratory (AFAL) in-house study of the durability testing of an iridium-plated storable rocket engine injector. AFAL Project Manager was Capt Kevin Benson.

This report has been reviewed and is approved for release and distribution in accordance with the distribution statement on the cover and on the DD Form 1473.

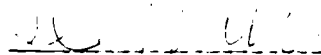


WAYNE L. PRITZ
Chief, Orbital Propulsion Section



ROBERT L. WISWELL
Chief, Space Propulsion Branch

FOR THE COMMANDER



DAVID J. OLKOWSKI, Maj, USAF
Deputy Chief, Liquid Rocket Division

REPORT DOCUMENTATION PAGE

1a REPORT SECURITY CLASSIFICATION UNCLASSIFIED		1b RESTRICTIVE MARKINGS	
2a SECURITY CLASSIFICATION AUTHORITY		3 DISTRIBUTION AVAILABILITY OF REPORT Approved for Public Release; Distribution is Unlimited.	
2b DECLASSIFICATION/DOWNGRADING SCHEDULE			
4 PERFORMING ORGANIZATION REPORT NUMBER(S) AFAL-TR-87-061		5 MONITORING ORGANIZATION REPORT NUMBER(S)	
6a NAME OF PERFORMING ORGANIZATION Air Force Astronautics Laboratory	6b OFFICE SYMBOL (if applicable) LKDB	7a NAME OF MONITORING ORGANIZATION	
6c ADDRESS (City, State and ZIP Code) Edwards AFB CA 93523-5000		7b ADDRESS (City, State and ZIP Code)	
8a NAME OF FUNDING SPONSORING ORGANIZATION	8b OFFICE SYMBOL (if applicable)	9 PROCUREMENT INSTRUMENT IDENTIFICATION NUMBER	
8c ADDRESS (City, State and ZIP Code)		10 SOURCE OF FUNDING NUMBERS	
		PROGRAM ELEMENT NO 62302F	PROJECT NO 3058
		TASK NO 00	WORK UNIT ACCESSION NO RA
11 TITLE (Include Security Classification) DURABILITY TESTING OF AN IRIIDIUM-PLATED STORABLE ROCKET ENGINE INJECTOR (U)			
12 PERSONAL AUTHOR(S) Benson, Kevin R.			
13a TYPE OF REPORT Special	13b TIME COVERED FROM 86/9 TO 87/3	14 DATE OF REPORT (Year, Month, Day) 87/9	15 PAGE COUNT 29
16 SUPPLEMENTARY NOTATION			
17 COSAT CODES		18 SUBJECT TERMS (Continue on reverse if necessary and identify by block number)	
FIELD	GROUP	SUB GROUP	
21	08	1	
21	08		
19 ABSTRACT (Continue on reverse if necessary and identify by block number) A series of hot firings were conducted at the Air Force Astronautics Laboratory (AFAL) to evaluate the durability of an iridium plated, like-doublet, storable rocket engine injector. The injector was designed for N ₂ O ₄ /MMH propellants and a chamber pressure of 1500 psia. Iridium plating failed to protect the injector face; however, valuable insights into the attack mechanism were gained. This report presents the results of AFAL's testing, including the analysis and evaluation of the injector orifice corrosion/erosion.			
20 SECURITY CLASSIFICATION OF ABSTRACT <input type="checkbox"/> UNCLASSIFIED <input checked="" type="checkbox"/> CONFIDENTIAL <input type="checkbox"/> SECRET <input type="checkbox"/> OTHER USERS		21 ABSTRACT SECURITY CLASSIFICATION UNCLASSIFIED	
22a AUTHOR NAME (Last, First, Middle Initial) Kevin R. Benson, Capt, USAF		22b TELEPHONE (Include Area Code) (805) 273-5542	22c OFFICE SYMBOL LKDB

TABLE OF CONTENTS

	<u>Page</u>
Introduction	1
Project Summary	2
Hardware Description	2
Facility	5
Instrumentation	6
Test Results	8
Damage Description	13
Observations	23
References	24



Accession For	
NTIS GRA&I	<input checked="" type="checkbox"/>
DTIC TAB	<input type="checkbox"/>
Unannounced	<input type="checkbox"/>
Justification	<input type="checkbox"/>
By _____	
Date _____	
Approved _____	
Special Agent _____	
Dist. _____	

A-1

LIST OF FIGURES

FIGURE	CAPTION	PAGE
1	Iridium Plated Injector Face	3
2	Injector Impingement Pattern	4
3	Experimental Area 1-52C Propellant Feed System	6
4	Thrust Chamber Assembly Instrumentation	7
5	Hot Fire Sequence Logic	8
6	STAR Tech Calorimeter Data	12
7	Injector Mixture Ratio Distribution	13
8	Damaged Oxidizer Orifice	14
9	Damaged Oxidizer Orifice With Iridium Tube	15
10	Damaged Oxidizer Orifice With Iridium Tube	16
11	Damaged Oxidizer Orifice With Melted Metal in Damaged Area	17
12	Oxidizer(lower left) and Fuel(upper left) Orifices	18
13	Damaged Oxidizer Orifice in Oxidizer Rich Region	19
14	Damaged Oxidizer Orifice in Oxidizer Rich Region	19
15	Damaged Oxidizer Orifice in Oxidizer Rich Region	20
16	Damaged Oxidizer Orifice in Oxidizer Rich Region	20
17	Damaged Fuel Orifice in Oxidizer Rich Region	21
18	Damaged Fuel Orifice in Oxidizer Rich Region	22
19	Boundary Layer Coolant Orifice	23

LIST OF TABLES

TABLE	TITLE	PAGE
1	Calorimetric Thrust Chamber Characteristics and Coolant Requirements	5
2	STAR Tech Iridium Plated Injector Test Conditions	9
3	STAR Tech Iridium Plated Injector Performance	10
4	STAR Tech Calorimeter Data	11

Introduction

The Air Force Astronautics Laboratory (AFAL) is currently pursuing development of a high performance, high chamber pressure, compact engine concept which uses Nitrogen Tetroxide (N₂O₄), and Monomethyl Hydrazine (CH₃NHNH₂), as propellants. This engine, designated the XLR-132, is designed to transfer Air Force payloads from low earth orbit to higher operational orbits.

A critical component required for development of this engine is a durable, high performance injector. Several electro-deposited nickel injectors were designed and tested by the Rocketdyne Division of Rocket International under the Breadboard XLR-132 contract. After several 10 second tests, damage caused by chemical attack, erosion, or a combination of the two was observed around the injector orifices. More severe damage was found following a 40 second firing. Several solutions were applied to alleviate the orifice erosion problem. Included among them were a fuel lag shut down, operation with cool N₂O₄, and chrome, rhenium, and gold platings applied to the injector face. These remedies did not prove effective at hindering orifice erosion.

Recent progress on a Small Business Innovative Research (SBIR) contract managed by AFAL has allowed Ultramet to develop a chemical vapor deposition process for iridium. This process was used to plate a Rocketdyne IP&D workhorse injector with iridium. The Rocketdyne iridium-plated injector was loaned to AFAL for evaluation of plating durability. This technical report describes the hardware, test procedure used to evaluate the iridium plating, and test results.

Project Summary

Four hot firings were conducted in February 1987 at the AFAL Rocket Motor Engine Complex, Experimental Area 1-52C. Following the fourth firing the injector was removed from the thrust stand for inspection. A Bausch and Lomb Stereomicroscope was used to inspect the injector face and showed that the iridium plating failed to protect the injector face. However, valuable insights into the attack mechanism were gained. Previous explanations proposed to account for the orifice damage relied on a mechanism involving reaction between N2O4 and nickel within the orifice. Inspection of the orifice damage which occurred on the iridium-plated injector suggests an attack mechanism step involving combustion gases and originating on the surface.

Hardware Description

Four primary pieces of hardware, designed and manufactured by Rocketdyne were used in this program: an IR&D like-doublet workhorse injector, an acoustic cavity ring, a water-cooled calorimetric thrust chamber, and a water-cooled calorimetric adapter section.

The injector tested on this program was a Rocketdyne-owned, IP&D injector. The injector consisted of a stainless steel body with two layers of 0.080 inch-thick electro-deposited nickel forming the face and fuel and oxidizer orifices. A chemical vapor deposition process was used to deposit a layer of iridium approximately 0.0008 inch thick on the injector face. A thin layer of iridium was also deposited within the injector orifices. A close-up of the iridium plated injector is shown in Figure 1.

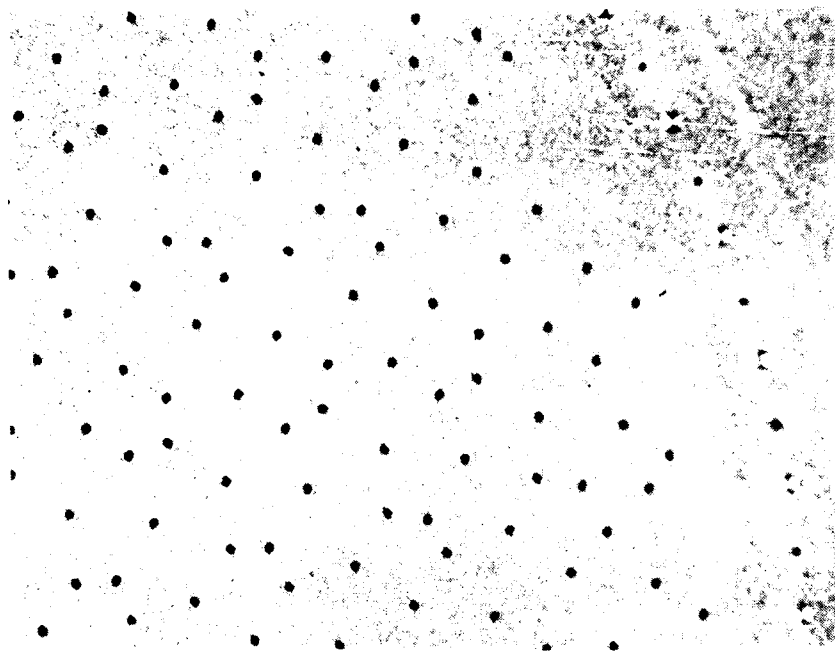


Figure 1. Iridium Plated Injector Face

The impingement pattern, which consists of like-on-like doublet elements, is shown schematically in Figure 2. Both oxidizer and fuel orifices are 0.0135 inch in diameter. The boundary layer coolant holes are 0.010 inch in diameter.

Acoustic damping of the injector was provided by a copper, water-cooled acoustic cavity ring with 12 gold plated cavity dividers. The acoustic cavity ring is also Rocketdyne-owned IR&D hardware.

The water-cooled calorimetric thrust chamber was designed and manufactured by Rocketdyne for AFAL's Storable Advanced Rocket Technology (STAR Tech) program. The calorimetric thrust chamber consists of a NARloy A liner and OFHC copper spacers brazed to a 347 stainless steel housing. The surface of the NARloy A liner exposed to hot gases is protected by electrodeposited gold.

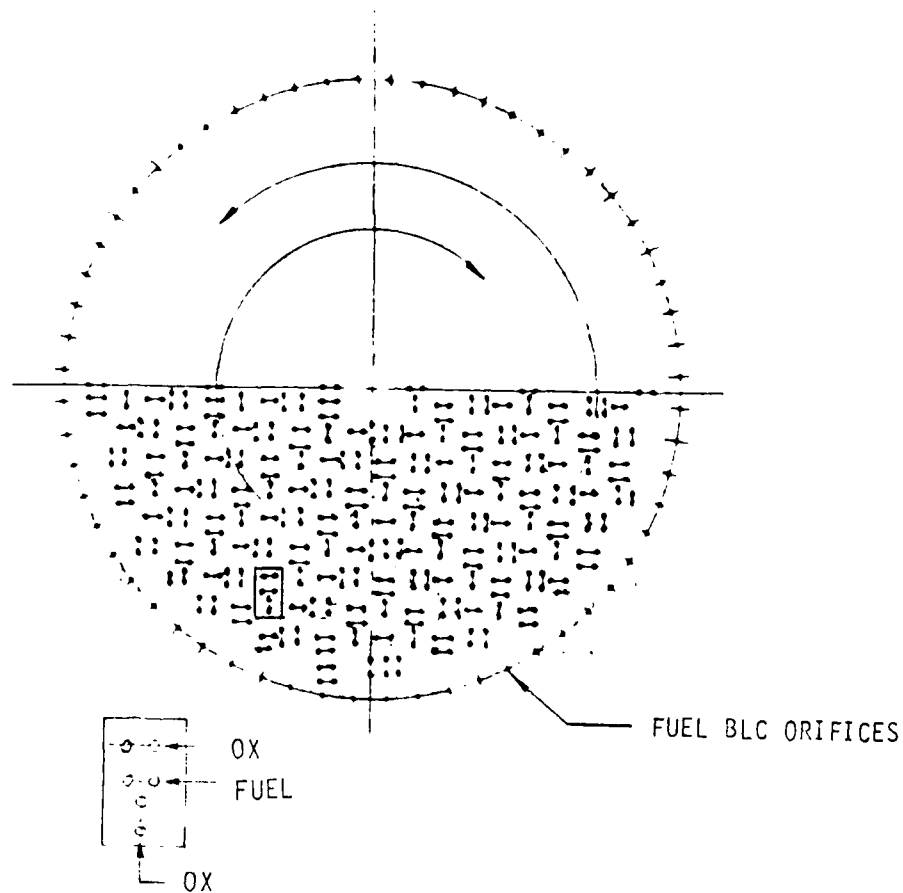


Figure 2. Injector Impingement Pattern

The thrust chamber has 10 radial coolant passages and each water-coolant inlet port has its accompanying exit port at 180 degrees, in the same axial plane. Table 1 describes the thrust chamber characteristics and coolant requirements. A more detailed description of the thrust chamber is available in Ref. 1.

A Rocketdyne-owned water-cooled adapter segment was used to attach the AFAL thrust chamber to the IR&D injector. The adapter segment is 2.5 inches in length and construction is similar to the calorimetric thrust chamber. The adapter segment has six radial coolant passages. Minimum required coolant flowrate to the adapter is 10 lbm/sec and the maximum is 20 lbm/sec.

Table 1. Calorimetric Thrust Chamber Characteristic and Coolant Requirements

COOLANT PORT NO.	FLOW CHAN. (NO.)	INTERNAL COOLED SURFACE, SQ. IN.	AVG AXIAL POSITION FROM THROAT, INCH	AVG EXPAN, A_{avg}/A_T	REQD WATER FLOW MINIMUM, lb/SEC	APPROX. COMBUSTION PRESSURE, PSIA
1	1	4.53	-3.10	-7.46	1.4	1500
2	2&3	6.39	-2.59	-6.96	2.0	1500
3	4&5	6.04	-1.99	-6.01	2.3	1500
4	6&7	5.50	-1.39	-4.68	2.6	1500
5	8&9	4.67	-0.79	-3.14	3.3	1500
6	10&11	2.61	-0.29	-1.68	3.4	1500
7	12&13	1.59	.10	1.01	3.8	1500
8	14&15	1.95	.49	1.33	1.8	378
9	16&17	2.91	.89	2.29	1.5	158
10	18&19	2.69	1.22	3.59	0.8	80

Exit location (from throat) 1.345 INCH
 Exit Diameter 2.67 INCH
 Exit Expansion Ratio A_e/A_t 4.42
 Total Coolant Flow
 Chamber 22.9 lb/s

Facility Description

All testing on this program was conducted at Experimental Area 1-52C. The propellant feed system in use at this area is shown schematically in Figure 3. Gaseous nitrogen, supplied at 6600 psig, is used for propellant tank pressurization, purging, and valve actuation.

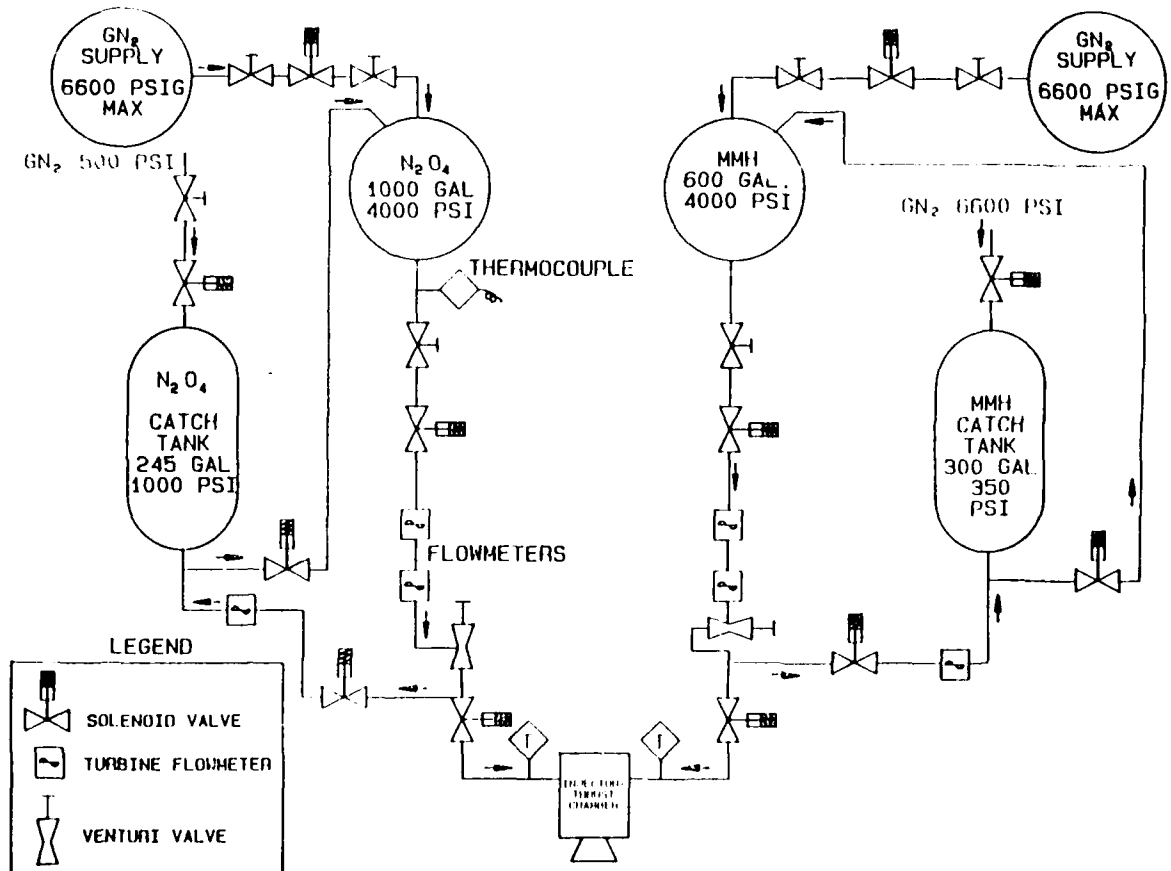


Figure 3. Experimental Area 1-52C Propellant Feed System

A 5000 lbf horizontal thrust stand was used for axial thrust measurement. Total thrust is measured by three parallel load cells, which are National Bureau of Standards traceable, and are accurate to 0.10% of full scale.

Thrust chamber de-ionized coolant water is supplied from two 300 cubic foot tanks at 2350 psig.

Instrumentation

Figure 4 shows a schematic diagram of the instrumentation used on this engine. Turbine flowmeters were used to measure the propellant flowrates.

Accuracy of both the fuel and oxidizer flowmeters was 0.5%. Two pressure transducers were used to measure chamber pressure. Water coolant flowrates to the acoustic cavity ring, the adapter segment, and the 10 thrust chamber coolant channels were measured with turbine flowmeters. Pressure and temperature of the inlet and outlet coolant water was measured on the acoustic cavity ring, and each of the thrust chamber coolant channels. Water coolant pressure and temperature was measured on the adapter segment inlet, but data for the outlet coolant water could not be obtained due to a limited number of data acquisition channels.

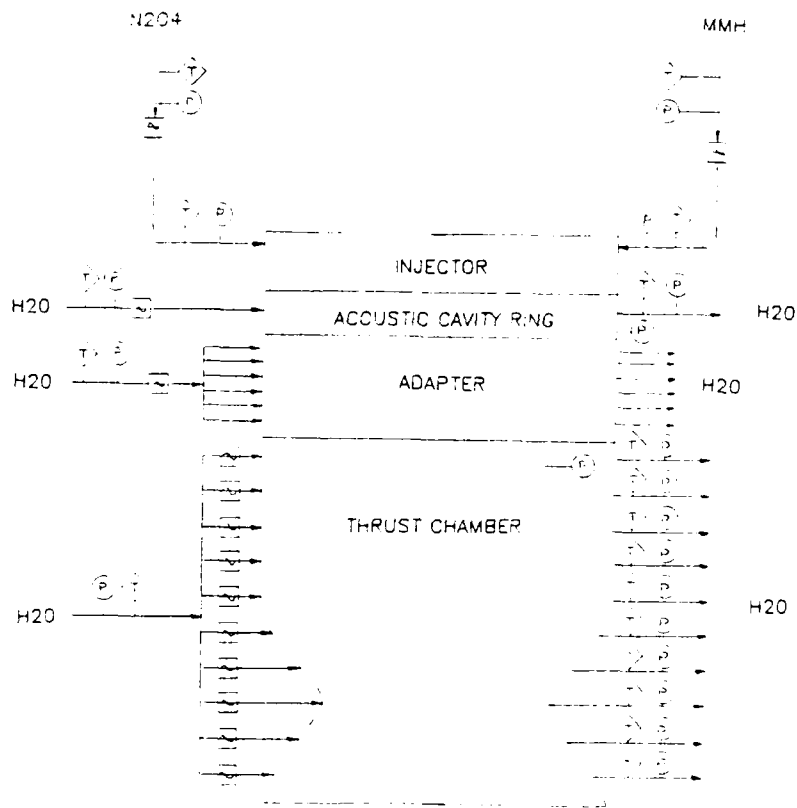


Figure 4. Thrust Chamber assembly Instrumentation

Test Results

A total of four tests were conducted at the Experimental Area. A typical hot fire sequence is shown schematically in Figure 5. The first two tests were short duration firings conducted to check out the facility feed system, data acquisition and control system, and hardware integrity. The third test was a 10 second duration firing, and the fourth test was a 40 second firing.

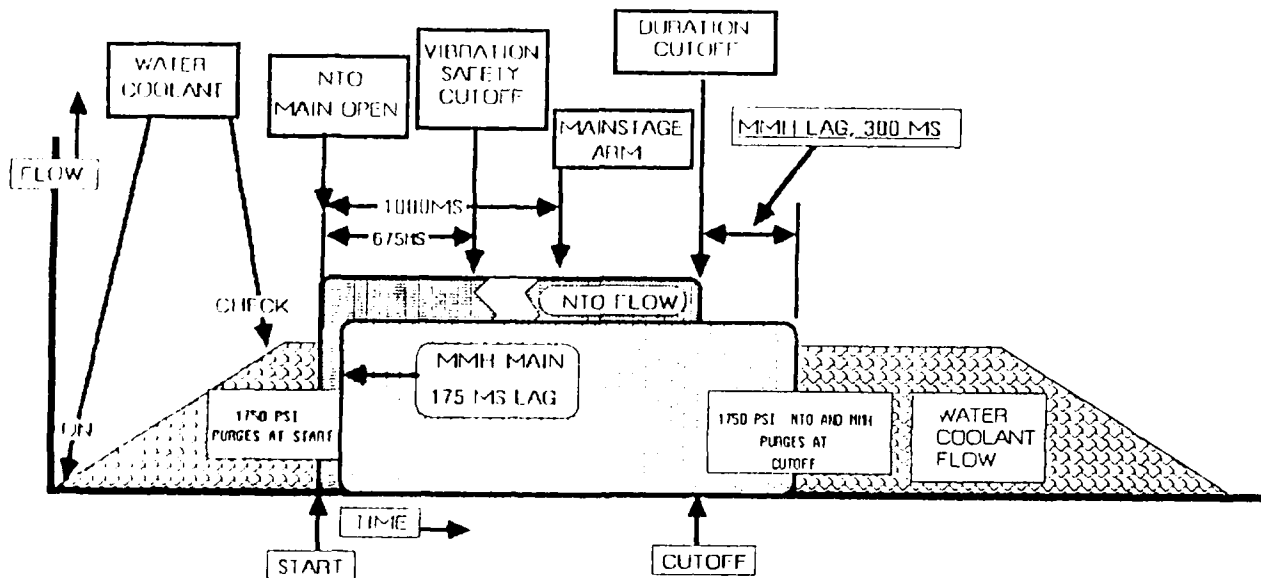


Figure 5. Hot Fire Sequence Logic

Table 2 presents the chamber pressure, mixture ratio, and propellant flowrates achieved on each firing. Chamber pressure was measured with two Taber strain gage pressure transducers. The difference between the two transducers was seldom more than 0.4%. The JANNAF method, [Ref. 2], for determining effective chamber pressure from wall static pressure measurements

was used to compute the chamber pressures listed in Table 2. The propellant flowrates listed in Table 2 represent a time average over the duration of the firing. During the test firing propellant flowrates rarely varied more than 0.3% from the average.

Table 2. STAR Tech Iridium Plated Injector

Test No.	1	2	3	4
Duration (s)	2	2	10	40
Cumulative Time (s)	2	4	14	54
Atmospheric Pressure (psic)	12.8	13.2	13.2	13.0
Chamber Pressure (psig)	1479	1470	1492	1502
Chamber Pressure (psia)	1492	1483	1505	1515
Oxidizer Flowrate (lbm/s)	7.18	7.28	7.36	7.42
Fuel Flowrate (lbm/s)	3.71	3.58	3.62	3.61
Mixture Ratio	1.94	2.03	2.03	2.06

Performance parameters calculated from the data collected during each test are listed in Table 3. Experimental values for chamber pressure, total propellant flowrate, and thrust were time averaged and then used to calculate C^* and I_{sp} . The throat area used for the C^* calculation was adjusted for thermal effects according to the JANNAF procedures given in Ref. 2. The

JANNAF procedure predicted a 0.36% increase in throat area due to thermal expansion. Also listed in Table 3 are theoretical values of C^* calculated with ODE according to the JANNAF procedures given in Ref. 3.

Table 3. STAR Tech Iridium Plated Injector performance

Test No.	1	2	3	4
Total Propellant Flowrate (lbm/s)	10.89	10.86	10.98	11.03
Facility Thrust (lbf)	2598	2589	2641	2646
CdA, fuel (in ²)	0.0443	0.0443	0.0443	0.0446
CdA, ox (in ²)	0.0689	0.0685	0.0694	0.0705
Isp (lbf s/lbm)	245.1	245.2	247.3	246.4
Measured C^* (ft/s)	5607	5589	5610	5621
Theoretical C^* (ft/s)	5788	5774	5776	5770
C^* Efficiency	96.9	96.8	97.1	97.4

Calorimetric data for the acoustic cavity ring and STAP Tech combustion chamber is given in Table 4. Calorimetric data for the 2.5 inch adapter segment was not obtained due to a shortage of data acquisition channels.

Table 4. STAR Tech Iridium Plated Injector

Test No.	1	2	3	4
AC Ring	57.6	84.0	84.2	78.1
Combustion Chamber Channel No.				
1	---	6.96	7.20-8.55	8.63-9.42
2	7.69	8.73	9.01-10.3	10.2-11.1
3	7.84	8.50	8.84-11.0	10.6-12.5
4	9.35	9.35	9.72-11.6	11.1-13.3
5	14.0	13.5	13.7-17.1	15.7-18.8
6	24.4	24.5	23.9-29.9	27.5-31.7
7	26.9	27.3	27.8-29.9	29.3-30.7
8	25.5	28.6	29.9-30.7	30.2-32.1
9	7.76	6.97	7.55	7.56
10	4.95	4.30	4.92	4.48

The main objective of this series of test firings was to evaluate the durability of the iridium plating. Following the fourth firing, the hardware was removed from the test stand and disassembled to permit detailed inspection of the injector face. Severe erosion was found on the oxidizer orifices. A detailed description of the orifice damage is given in the following section.

Table 3 presents performance data which was acquired during the test firings. As shown in Table 3, the C^* efficiency was approximately 97%, and remained high despite the orifice erosion. This data compares favorably with the C^* performance data acquired during Breadboard XLR-132 testing of a similar like-doublet injector. Measured C^* efficiencies for the Breadboard XLP-132 injector were 97-98% [Ref 4].

Propellant flowrates and pressure drop across the injector manifold were used to calculate the injector flow resistance. The results for each test are presented as CDA values in Table 3. The CDA values for both the oxidizer and fuel manifolds remained fairly constant throughout the test series, indicating that flow resistance across the injector was not changed significantly by erosion of the injector orifices.

Calorimetric data obtained during each test firing is presented in Table 4. The STAP Tech combustion chamber was designed to reach thermal equilibrium in less than 0.5 seconds. Inspection of the calorimeter data for tests 3 and 4 revealed increasing heat flux throughout the duration of the firing. In addition, heat flux at the start of Test 4 is close to the high heat flux obtained at the end of Test 3. To illustrate this phenomena more clearly, Figure 6 shows calorimetric data for selected channels plotted as a function of time.

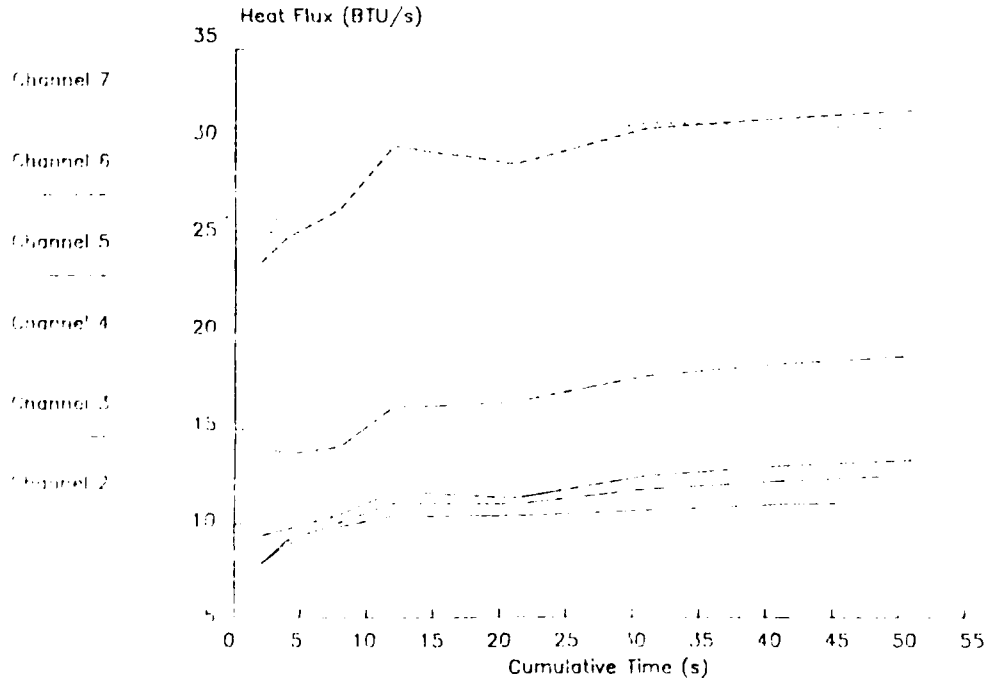


Figure 6. STAP Tech Calorimeter Data

Disassembly and inspection of the hardware following Test 4 revealed increased surface roughness of the combustion chamber due to metallic deposits. The deposit locations correspond to channels where increased heat flux was observed. A possible explanation is that increased surface roughness due to metallic deposits caused a corresponding increase in the heat transfer coefficient. The deposited material was probably nickel which eroded away from the injector face. Similar phenomena was observed on the Breadboard XLR-132 program.

Damage Description

Two distinct regions of damage can be identified on the injector face. These two regions correspond closely to the fuel-rich and oxidizer-rich regions of the injector. The oxidizer-rich region occurs in the center and extends out approximately 1.54 inches. The fuel rich region extends from a radius of 1.54 inches to 1.75 inches. Figure 7 shows the location of the oxidizer-rich and fuel-rich regions.

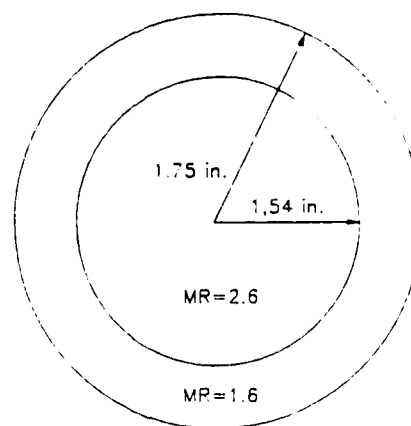


Figure 7. Injector Mixture Ratio Distribution

Damage throughout the entire injector face is always more severe on the oxidizer orifices. However, within the fuel-rich region damage to the oxidizer orifices is especially severe. The damage to the oxidizer orifices in this region extends deeper and wider than that which has occurred on similar oxidizer orifices located in the oxidizer rich region. Figures 8 and 9 show the pattern of attack which is typical on oxidizer orifices in the fuel rich region. The damage typically extends over a region from the oxidizer lip out to 0.003-0.007 inch with the a depth of damage usually 0.006-0.013 inch. The erosion undercuts the surface, as can be seen in Figure 8 from the 8 to 12 o'clock position.

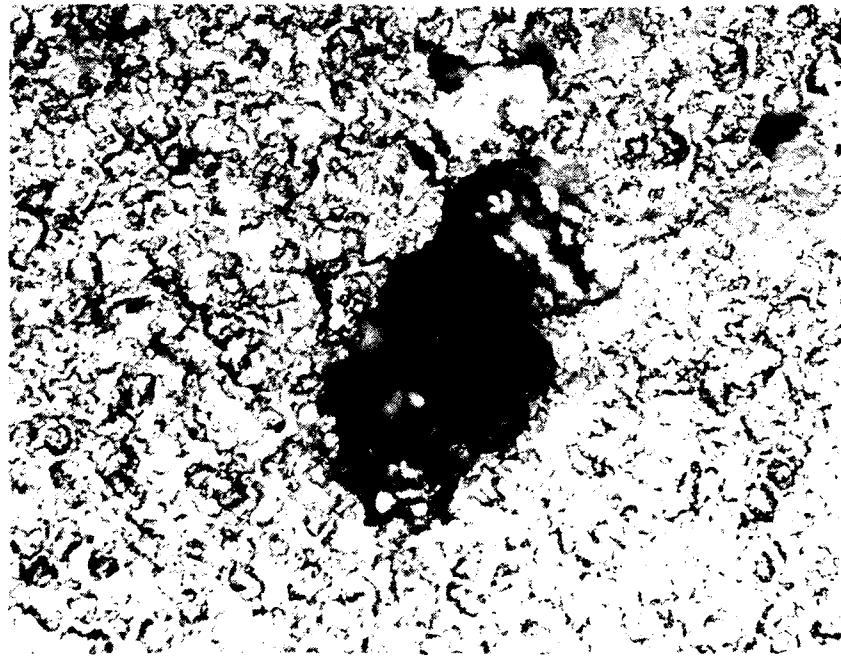


Figure 8. Damaged Oxidizer Orifice

A unique phenomenon which has been observed in the fuel rich region of this injector is the existence of free standing iridium tubes within the damaged oxidizer orifices. In Figure 9, part of an iridium tube is evident at the 9 o'clock position. It appears that the nickel substrate is preferentially attacked, leaving a free standing tube, or wall, of iridium in the orifice. This phenomenon was not observed on similar injectors which had been coated with chromium, rhenium, or gold.

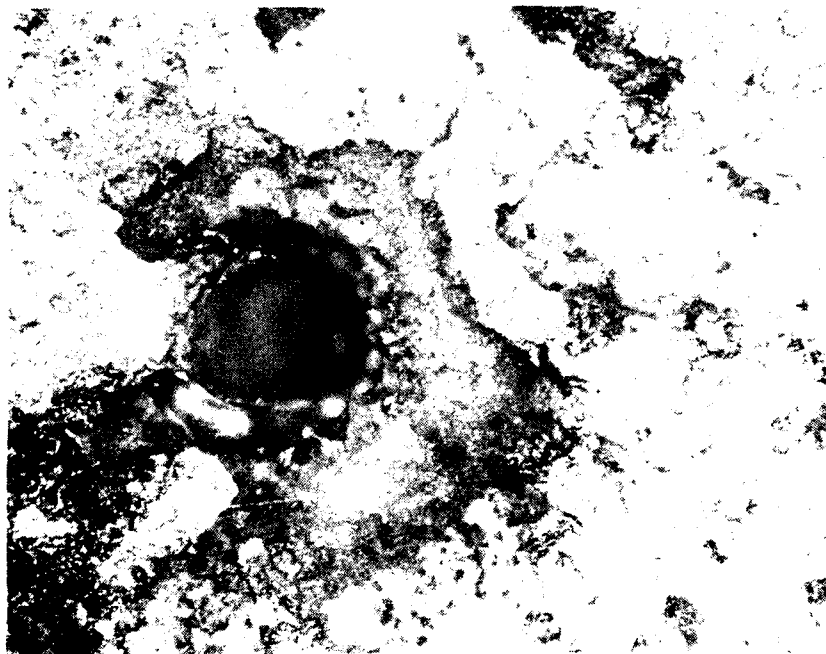


Figure 9. Damaged Oxidizer Orifice with Iridium Tube

In orifices where part, or all, of the iridium tube has been removed, sharp, jagged edges are observable. This is evident in Figure 9 at 9 o'clock and in Figure 10 at 4 o'clock. This would suggest that removal of the iridium

tube was due to shear stress from the flowing propellant, rather than by chemical attack.

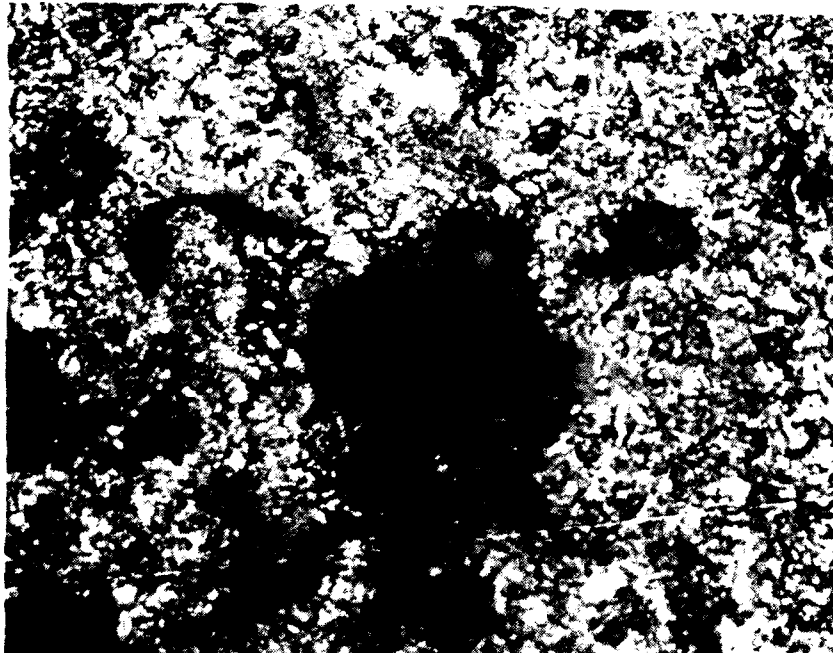


Figure 10. Damaged Oxidizer Orifice with Iridium Tube

Another interesting phenomenon observed on the oxidizer orifices in the fuel-rich region is the existence of molten metal in the damaged area. The molten material is distinguishable due to its smooth surface and apparent lack of grain boundaries (see Figures 9 and 11). It is most likely that the molten metal is nickel which melts at 2651F, as opposed to iridium which melts at 4438F. A possible explanation of this phenomena is that melting occurred due to local heating from an extremely exothermic reaction.

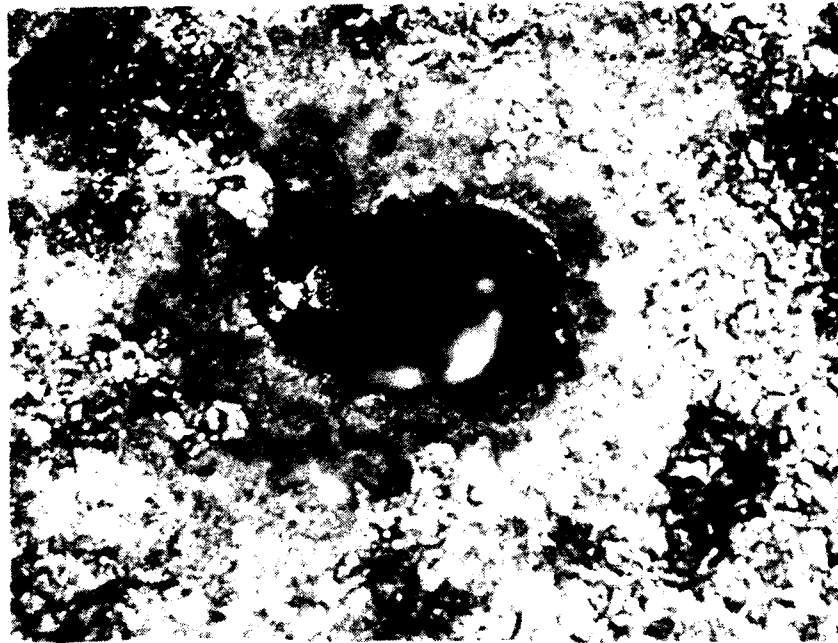


Figure 11. Damaged Oxidizer Orifice With Melted Metal in Damaged Area

On some of the oxidizer orifices in the fuel-rich region damage is less severe. Figure 12 shows an oxidizer (lower left), and fuel orifice (upper right). The oxidizer orifice exhibits features typical of damaged oxidizer orifices in the fuel rich region. Molten metal is noticeable in the damaged area, and an undercut surface is evident. However, the damage has not progressed as far as it has on other oxidizer orifices in this region. The fuel orifice in Figure 12 also shows some damage at the 3 o'clock position. Although it's not clear in the photo, the iridium plating within the fuel orifice has cracked at 9 o'clock. The crack is approximately 0.007 inch deep.



Oxidizer (lower left) and Fuel (upper right) Orifices

Damage in the injector's oxidizer rich region is less severe than that which has occurred in the fuel rich region. Oxidizer orifices are preferentially attacked, although fuel orifices also show signs of damage. Damage is usually confined to a narrow region surrounding the orifice and has eaten down behind the iridium which was plated within the orifice. Figures 13, 14, and 15 illustrate the predominate pattern and severity of attack to oxidizer orifices in the center region. Figure 16 shows an oxidizer orifice, located near the center, which has been more severely attacked. The iridium plating in the orifice has been torn away, and local melting has occurred from 6 to 9 o'clock.

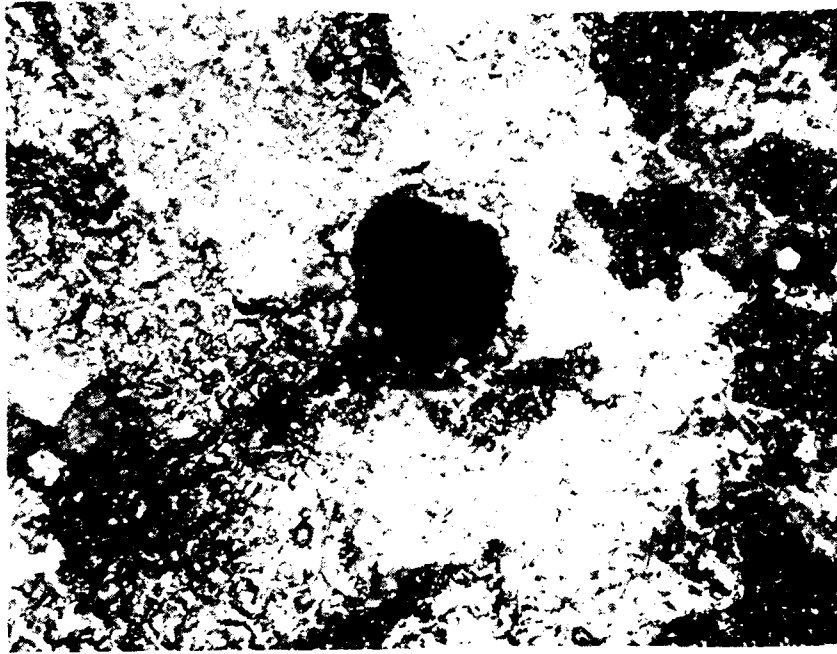


Figure 13. Damaged Oxidizer Orifice in Oxidizer Pich Region

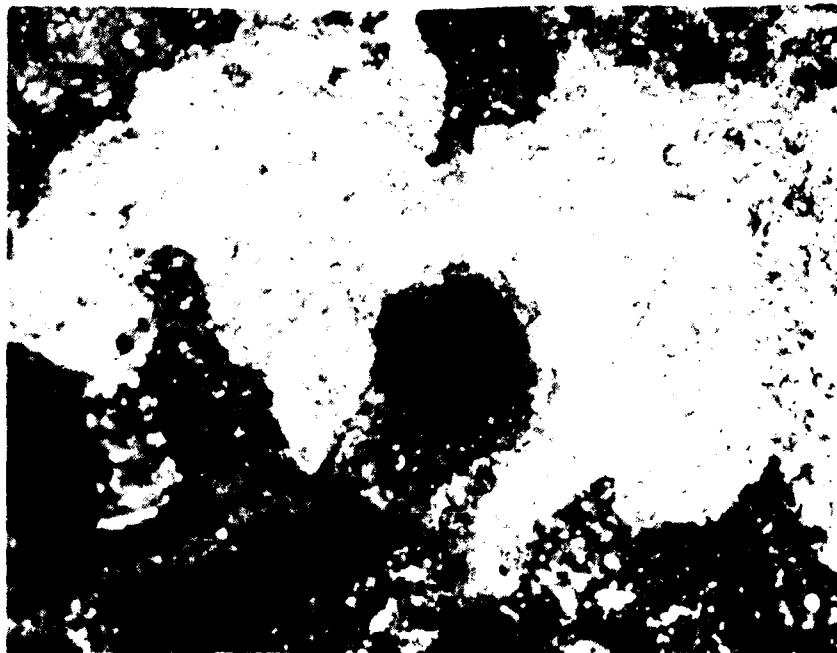


Figure 14. Damaged Oxidizer Orifice in Oxidizer Pich Region

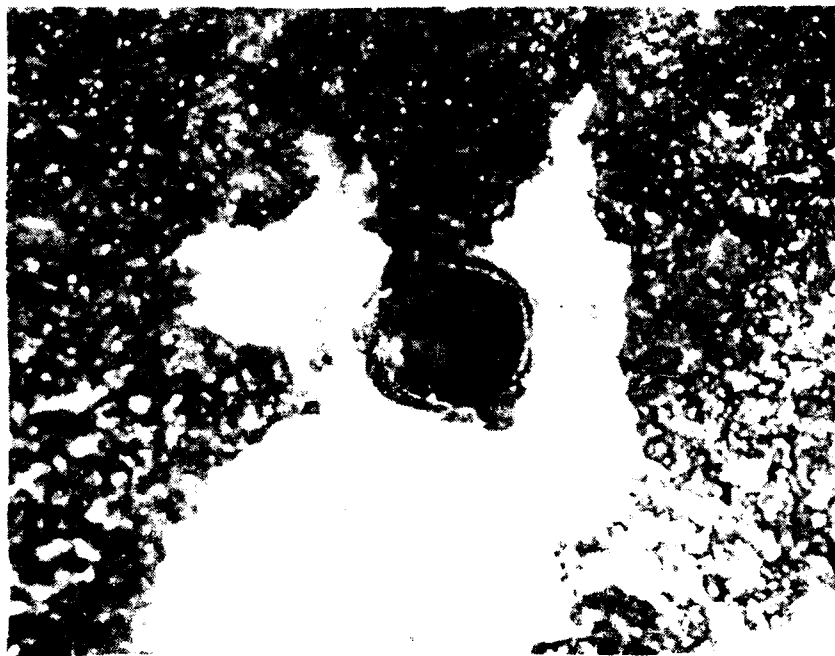


Figure 15. Damaged Oxidizer Orifice in Oxidizer Pich Region

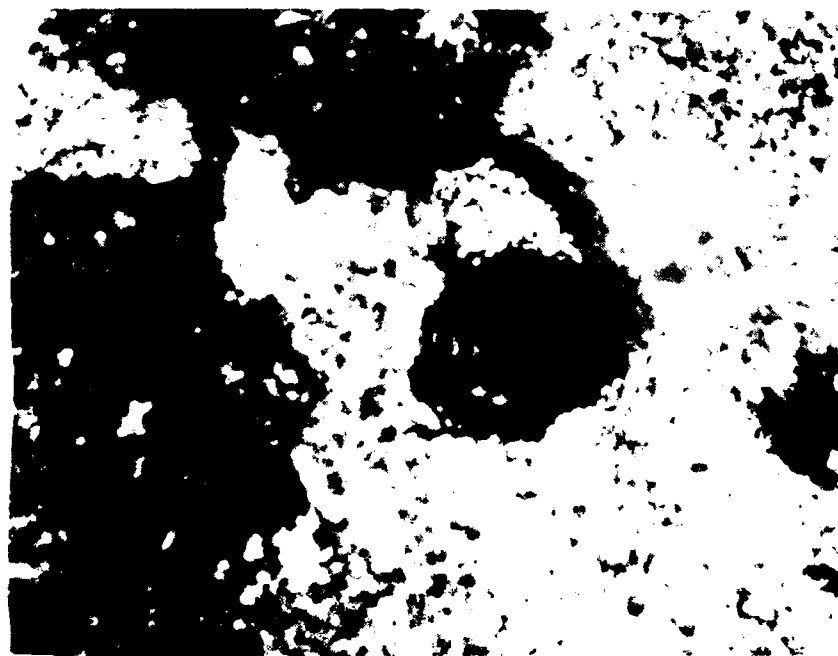


Figure 16. Damaged Oxidizer Orifice in Oxidizer Pich Region

Fuel orifices in the oxidizer rich center region also exhibit signs of attack. On the fuel orifice in Figure 17 pitting of the orifice lip is evident. Figure 18 shows a fuel orifice which has been attacked at the 6 o'clock position. The damage on fuel orifices is similar to that observed on the oxidizer orifices in this region, but is not as severe.

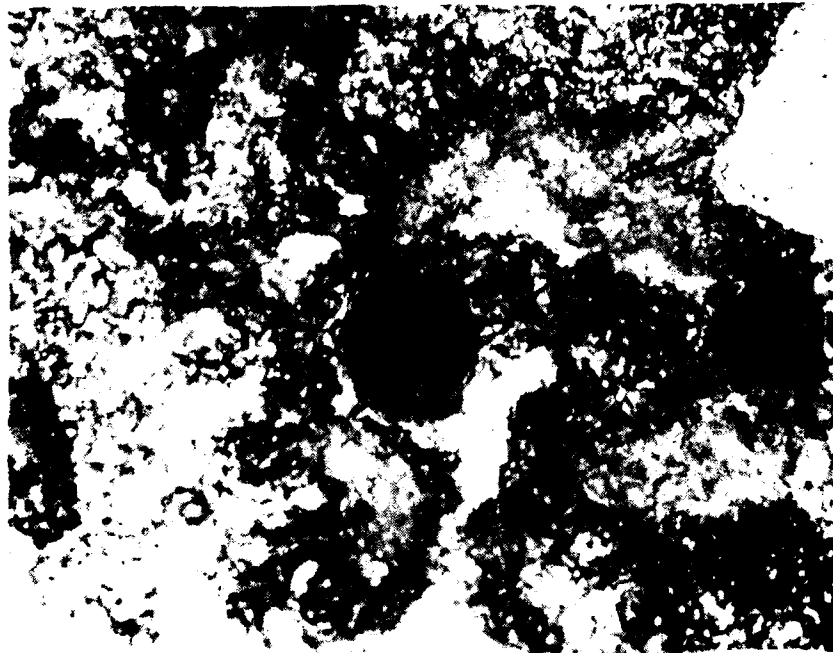


Figure 17. Damaged Fuel Orifice in Oxidizer Rich Region

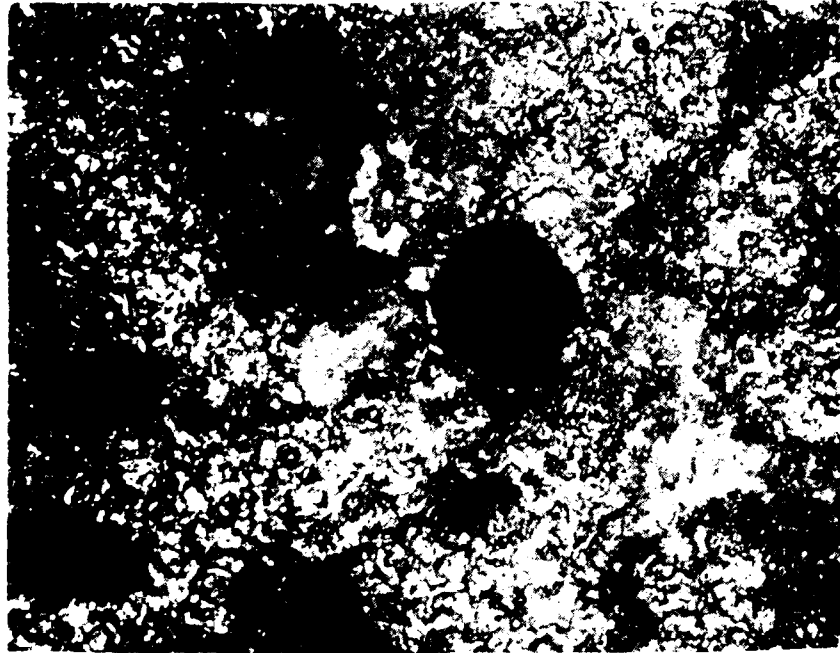


Figure 18. Damaged Fuel Orifice in Oxidizer Rich Region

In contrast to the fuel and oxidizer damage, all of the boundary layer coolant orifices, as well as the area immediately surrounding them, are in good condition. A typical boundary layer coolant orifice is shown in Figure 19.

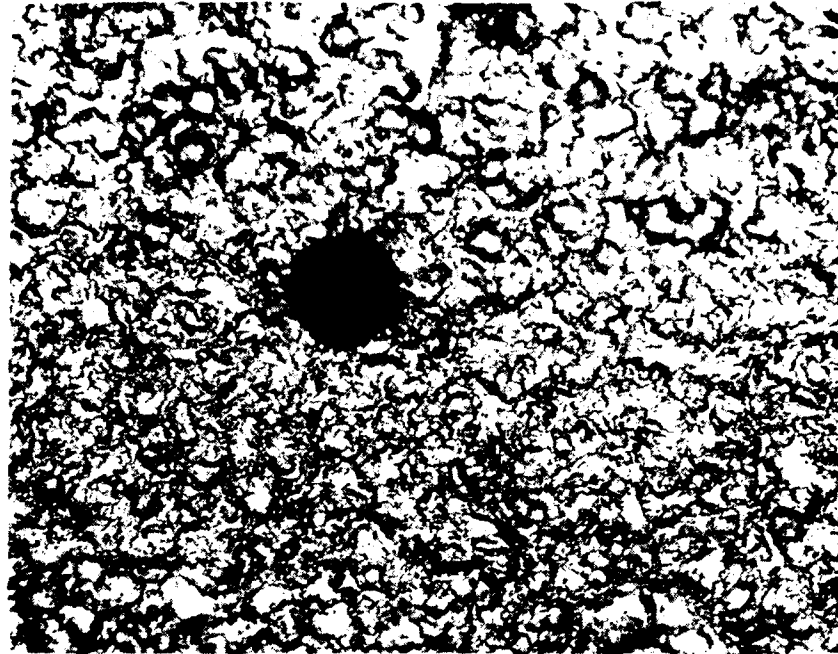


Figure 19. Boundary Layer Coolant Orifice.

Observations

The following observations have been made during our examination of the damaged injector:

- 1) Both fuel and oxidizer orifices exhibit signs of damage, however, damage to the oxidizer orifices is always more severe than the fuel orifices.
- 2) Damage has progressed farthest on oxidizer orifices in the fuel-rich region of the injector.

- 3) Other than a correlation of damage severity to mixture ratio zone, there was no apparent orientation with the physical characteristics of the injector, such as the orifice pattern, propellant inlets, or acoustic cavity locations.

REFERENCES

1. Neilsen, T.I., Huebner, A.W., and McMillion, R.L., STAR Tech Engine Operations Manual, AFRPL TR-85-063, Air Force Rocket Propulsion Laboratory, Edwards Air Force Base, California, June 1986.
2. JANNAF Rocket Engine Performance Test Data Acquisition and Interpretation Manual, CPIA Publication 245, April 1975.
3. JANNAF Rocket Engine Performance Prediction and Evaluation Manual, CPIA Publication 246, April 1975.
4. Johnson, J.R., Treinen, T.J. and McMillion, R.L., Advanced Spacecraft Engine Components-Breadboard XLR-132, AFRPL-TR-86-086, Air Force Astronautics Laboratory, Edwards Air Force Base, California, June 1987.

END
DATE
FILMED
DTIC
4/88